Surg Endosc (2013) 27:3280–3287
DOI 10.1007/s00464-013-2906-7

Transrectal quantitative shear wave elastography in the detection and characterisation of prostate cancer

Sarfraz Ahmad · Rui Cao · Tomy Varghese · Luc Bidaut · Ghulam Nabi

Received: 18 November 2012 / Accepted: 12 February 2013 / Published online: 23 March 2013

Abstract
Background Shear wave imaging (SWI) is a new ultrasound technique whose application facilitates quantitative tissue elasticity assessment during transrectal ultrasound biopsies of the prostate gland. The aim of this study was to determine whether SWI quantitative data can differentiate between benign and malignant areas within prostate glands in men suspected of prostate cancer (PCa).
Methods We conducted a protocol-based, prospective, prebiopsy quantitative SWI of prostate glands in 50 unscreened men suspected of prostate cancer between July 2011 and May 2012. The ultrasound image of whole prostate gland was arbitrarily divided into 12 zones for sampling biopsies, as is carried out in routine clinical practice. Each region was imaged by grey scale and SWI imaging techniques. Each region was further biopsied irrespective of findings of grey scale or SWI on ultrasound. Additional biopsies were taken if SWI abnormal area was felt to be outside of these 12 zones. Quantitative assessment of SWI abnormal areas was obtained in kilopascals (kPa) from abnormal regions shown by SWI and compared with histopathology. Sensitivity, specificity, positive and negative predictive values, and likelihood ratios were calculated for SWI (histopathology was a reference standard).
Results Fifty patients, with a mean age of 69 ± 6.2 years, were recruited into the study. Thirty-three (66 %) patients were diagnosed with PCa, while an additional 4 (8 %) had atypia in at least one of the 12 prostate biopsies. Thirteen (26 %) patients had a benign biopsy. Data analysed per core for SWI findings showed that for patients with PSA <20 μg/L, the sensitivity and specificity of SWI for PCa detection were 0.9 and 0.88, respectively, while in patients with PSA >20 μg/L, the sensitivity and specificity were 0.93 and 0.93, respectively. In addition, PCa had significantly higher stiffness values compared to benign tissues (p <0.05), with a trend toward stiffness differences in different Gleason grades.
Conclusion SWI provides quantitative assessment of the prostatic tissues and, in our preliminary observation, provides better diagnostic accuracy than grey-scale ultrasound imaging.

Keywords Prostate cancer · Shear wave elastography · Prostate

S. Ahmad · R. Cao · G. Nabi
Academic Section of Urology, Division of Cancer, Medical Research Institute, Ninewells Hospital, University of Dundee, Dundee DD1 4HN, UK

T. Varghese
Department of Medical Physics, University of Wisconsin–Madison, Madison, WI 53705, USA

L. Bidaut
Clinical Research Imaging Facility, Division of Imaging and Technology, Medical Research Institute, Ninewells Hospital, University of Dundee, Dundee DD1 4HN, UK

G. Nabi (✉)
Division of Imaging and Technology, Medical Research Institute, Medical School, University of Dundee, Dundee DD1 9SY, UK
e-mail: g.nabi@nhs.net

Men suspected of having prostate cancer (PCa) are currently offered a standard grey-scale (B-mode) transrectal ultrasound (TRUS)-guided prostate biopsy [1]. Standard grey-scale TRUS imaging based on increased brightness with respect to the strength of the echo intrinsically falls short of making a reliable differentiation between cancer and normal hyperplasia of the gland [2]. Accordingly,

current transrectal ultrasound imaging technology is essentially limited to measuring prostate volume and guiding needles into the region of interest (ROI) as per the standard biopsy protocol, and not surprisingly it has been reported to have poor diagnostic accuracy for cancer foci [3–5]. An ideal imaging technique should accurately locate cancer foci in the prostate gland and guide the needle to the lesion of interest. Clinically, this will reduce/preclude unnecessary biopsies from normal areas of the prostate, thereby reducing both cost and patient morbidity. Furthermore, accurate localisation of cancerous areas within the prostate gland will have an enormous implication for focal therapy for PCa.

Prostate cancer in routine clinical practice is suspected by an elevated level of serum prostate-specific antigen level (PSA) and/or an abnormal digital rectal examination. A digital rectal examination (DRE) for suspected PCa relies on the perceived differences in the stiffness of cancer and the normal prostate. This relationship of stiffness variation is quantified by Young's modulus, which is defined as $E = \sigma/\varepsilon$, where σ is the applied stress and ε is the strain (the ratio of the resultant deformation of the tissue over the original reference length of the medium). This is also known as stiffness or elasticity. Malignant lesions tend to be stiffer than benign tissue [6]. This reflects a change in cell density due to unregulated proliferation of malignant cells [6]. Such anatomical changes due to disease progression can be imaged using new techniques such as quasistatic elastography, vibration sonoelastography, acoustic radiation force generated by ultrasound pulse sequences, and real-time shear wave velocity imaging [3]. The measurement of tissue stiffness using ultrasound elastography is based on the basic relationship in physics that governs deformation in tissues and has been proposed as a means of enhancing cancer detection rates in both the breast and the prostate [3, 5, 7, 8]. However, most clinical ultrasound elastography systems are based on a quasistatic deformation technique, whose major drawbacks relate to dependency on operator skills, reproducibility, and subjectivity due to changes in the applied deformation among different studies [6]. Recent improvements in ultrasound technology, in particular, the introduction of an innovative shear wave elastography technique termed shear wave imaging (SWI), are aimed at overcoming these drawbacks. Crucially, SWI is intrinsically quantitative and has much less operator dependence, thus providing the potential for effective improvement of cancer detection and characterisation [9, 10].

SWI technology has been described in detail by Bercoff *et al.* [11, 12]. Briefly, the process involves generation of shear waves in tissue using acoustic radiation force generated by multiple focused ultrasound beams. Two quasi-planar shear wave fronts are generated within the tissues and propagate within tissues and organs under examination. As these waves propagate through tissue, the shear wave velocity (V_s) changes as it is affected by stiffness variations, with the wave propagating faster in stiffer tissues than in softer tissues [13]. An ultrafast imaging system then acquires successive raw radiofrequency signals at a high frame rate (up to 20,000 frames per second) using plane wave insonification. Post-processing of the high-frame-rate radiofrequency data enables extraction of the related quantitative information [e.g., the elasticity index, expressed in kilopascals (kPa)] [14], the shear wave velocity V_s (m/s), or Young's modulus (kPa) for each pixel. This information is colour-coded and overlaid on the B-mode anatomical image in real time. Shear wave velocity images provide quantitative information on stiffness changes without limiting assumptions on tissue density that may introduce errors in the shear and Young's modulus estimated. Further details about the principles of elastographic imaging and the differences between strain and shear wave imaging approaches have been discussed previously [13, 15–22]. SWI has been implemented for both ultrasound and magnetic resonance (MR) applications. Currently, SWI is the only elastographic approach that is able to provide quantitative local tissue elasticity information in real time [23].

The present prospective study is aimed at determining (1) the correlation of SWI-derived elasticity measurements (minimum, maximum, and mean stiffness with SD) of prostate areas with TRUS-guided histology findings, and (2) the diagnostic accuracy of SWI when compared with protocol-based, grey-scale, ultrasound-guided systematic biopsies of the prostate in men suspected of having PCa.

Materials and methods

Study population

A prospective protocol-driven study with prior ethical and institutional approval (REC Ref 11/AL/0359) was designed to assess the feasibility of SWI in the detection of PCa in referred patients with suspected disease. The indications for a prostate biopsy were abnormal PSA (>4 μg/L), ± abnormal DRE and patients on active surveillance or with a previous abnormal prostate biopsy, e.g., prostate intraepithelial neoplasia (PIN) and atypical small-cell acinar proliferation (ASAP).

TRUS, SWI, and prostate biopsies

Data were obtained using the Aixplorer® ultrasound system (SuperSonic Imagine, Aix-en-Provence, France). A transrectal endocavity transducer SE 12-3 was used to scan the

prostate (for both grey-scale ultrasound and SWI). Imaging was performed along the axial and sagittal planes, from the seminal vesicles to the apex of the gland. After volume measurement, the prostate was divided into 12 zones as a template for both imaging and prostate biopsy (Fig. 1). The grid shown in Fig. 1 is a rough guide for directing needles during sampling of the prostate gland and does not appear in real time. Two orthogonal images were obtained for each zone for grey scale and SWI using the same machine and setup (Fig. 2). Because the field of view with SWI was not wide enough to evaluate the entire prostate, the right and left lobes were imaged separately. For SWI, no pressure was applied on the prostate while the probe maintained contact for at least 15 s to ensure the acquisition of stable SWI data. The images were stored and quantitative analysis was carried out at a later date by an independent researcher who was not involved in the acquisition of the imaging data. This offline protocol minimised disruption with the clinical workflow in a busy outpatient biopsy clinic.

Each study participant had at least one biopsy from each of the 12 zones shown in Fig. 1, obtained using only grey-scale imaging, following the clinical work flow in a current contemporary clinical practice. Additional biopsies (one biopsy per abnormality) were obtained from abnormal areas (well-defined area of high stiffness colour-coded as red or nonblue on the machine screen) seen on SWI, if that ROI had not already been sampled by the standard 12-core technique (Fig. 1). Images (from red to blue for high to low stiffness, respectively) for each region were stored digitally and the quantitative measurement of the stiffness was performed (Fig. 2). During biopsies, researchers were provided information on only the stiffer (colour-coded as red) and softer (colour-coded as blue) areas without any quantitative measurements. The core biopsies obtained in real time from the ROI seen on SWI were then correlated with the histopathology findings. Tissue stiffness was expressed as Young's modulus (kPa) or simply as the ratio of stress per unit area to the strain (the ratio of the resultant deformation of the tissue over the original reference length of the medium) [21]. Tissue biopsy specimens were processed and examined independently by uropathologists blinded to the quantitative stiffness data. Histological grading was performed through an established Gleason scoring mechanism [24] and correlated with quantitative stiffness data.

Statistical analysis

The primary outcomes were reliability of SWI in differentiating benign and malignant prostate tissues and determining sensitivity and specificity of SWI-guided prostate biopsies when compared to standard TRUS-guided biopsies using grey-scale B-mode ultrasound. The data were analysed by a third party not involved in the TRUS biopsy procedure. The patients were categorised according to pathology results. The PCa patients were divided into two groups: PSA 4–20 μg/L and PSA >20 μg/L. The study cohort was an unscreened population, and it was arbitrarily felt (based on clinical experience and reported literature) that a cutoff of 20 would help us identify a group of patients (PSA <20) with clinically localised disease. The

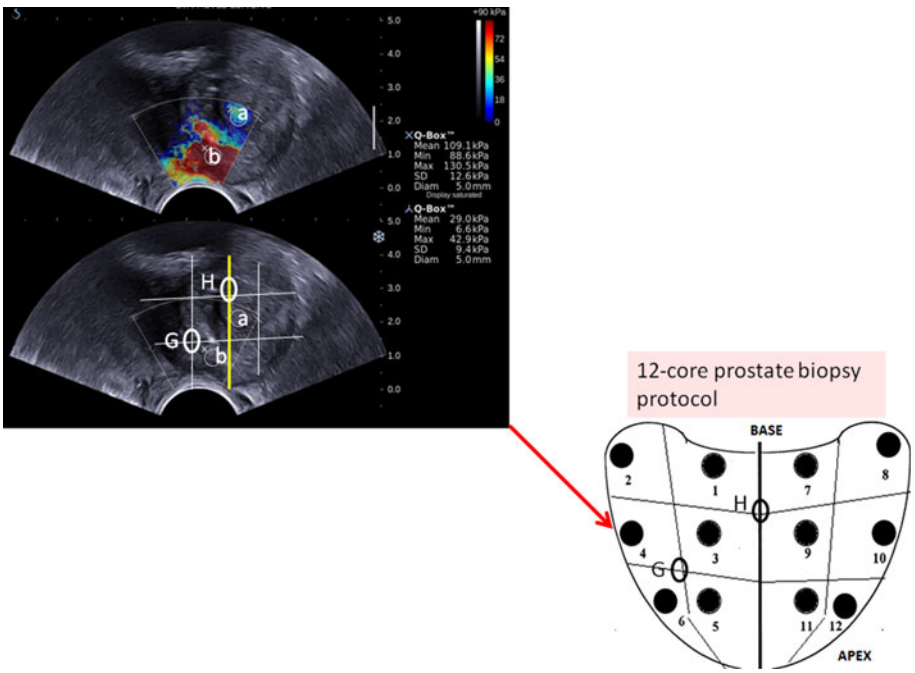

Fig. 1 Ultrasound image of prostate divided into 12 regions for biopsy and subsequent correlation between SWI images and biopsies. *Note* abnormal (**b**) and normal (**a**) SWI images. Each region was imaged and correlated with the histopathology of the biopsy. Also, *note* the stiffness quantification *labels* on the *right side* of the image along with scale of stiffness (*top right*). G&H represent SWI detected abnormal areas that felt outside the 12 regions of the prostate template used in 12 core biopsy protocol

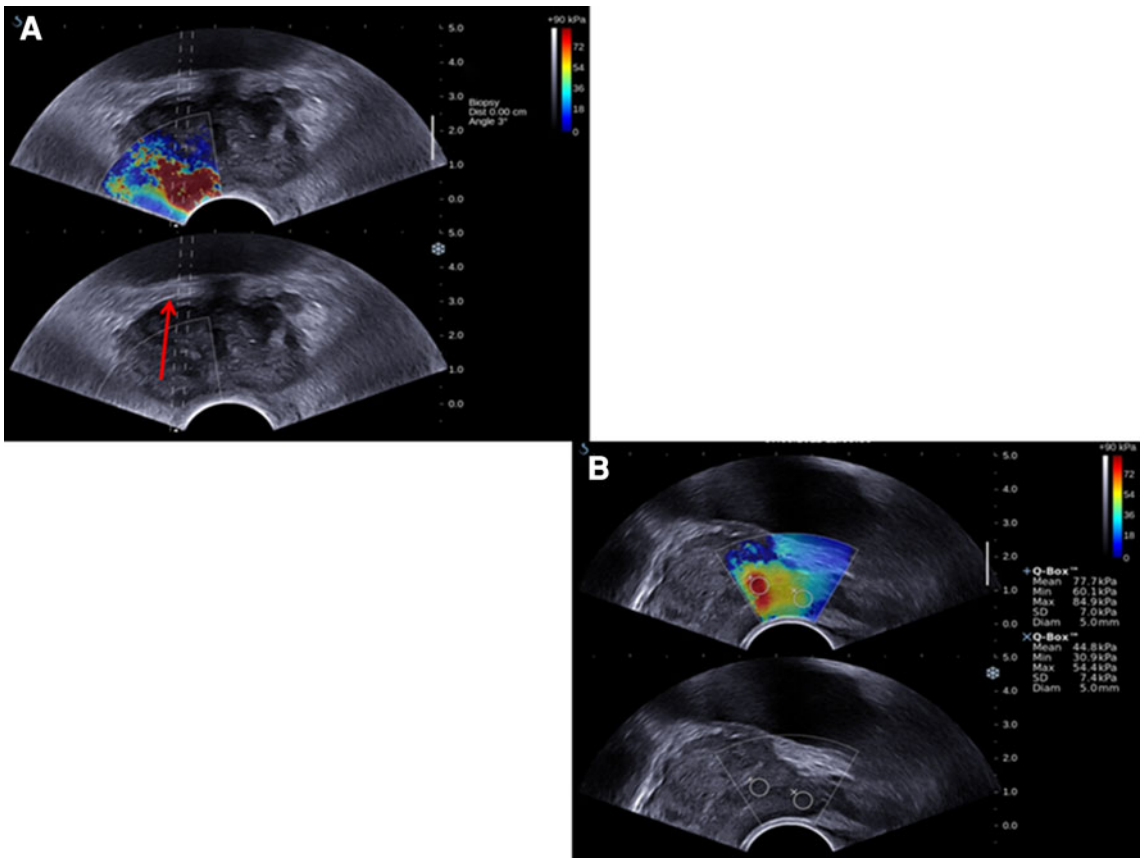

Fig. 2 Comparison of grey-scale TRUS (B-mode; *bottom row*) and overlaid SWI images (*top row*). Representative images showing abnormal area (*red* indicates high stiffness) detected only by SWI. **A** *Note* the *red arrow* showing needle guide for the real-time biopsy of an abnormal area seen only on SWI images. The abnormal area was Gleason 3+4 adenocarcinoma on histopathology. **B** *Note* the quantitative assessment of abnormal areas using cursor (*circle*) and instantaneous values displayed on the right of the image on the machine's screen. A *multicolour scale* on the *top right* of the images indicates measurement scale in kPa (Color figure online)

SWI findings were quantified and compared with histological results. Young's modulus (kPa) was compared between malignant and benign tissues. A paired two-sample Student *t*-test was used to calculate the *p* value, which if <0.05 was considered as significant.

Results

Correlation of prostate gland stiffness with histopathology results

The quantification of stiffness within the prostate gland using SWI [Young's modulus (kPa)] was performed and matched with histopathological results (Fig. 3) for each ROI. The mean Young's modulus (±SD) values of the prostate areas with histopathologically confirmed PCa (133.7 ± 57.6 kPa) were much higher than those of benign areas (74.9 ± 47.3 kPa) and PIN/atypia (83.3 ± 38.6 kPa). Mean Young's modulus values of PCa were statistically significant and higher when compared with mean Young's modulus values for the benign patients ($p = 0.002$). However, a separate comparison of the mean Young's modulus values of PCa with individual categories of the patients in the benign group (i.e., with normal parenchyma, chronic inflammation, acute inflammation, and atrophic parenchyma) was not statistically significant, mainly because of the small numbers of patients in individual categories. Similarly, the difference between stiffness of PIN/atypia and the benign cases was not statistically different, even though the mean Young's modulus in the former group (83.3 ± 38.6 kPa) was higher than that in the latter (74.9 ± 47.3 kPa). On the basis of histopathology results, the patients were divided into three groups: (1) all prostate cancer, (2) all benign, and (3) PIN/atypia. The mean Young's modulus of each of the patients in these three groups is illustrated in a whisker plot in Fig. 4. Note that more than one core biopsy specimen were positive for cancers in few patients. Young's modulus for the highest grade of reported cancer was recorded and is shown in Fig. 5. The presence of higher Gleason scores in the histopathology results is a clinical significance and influences the decision-making of the individual patient.

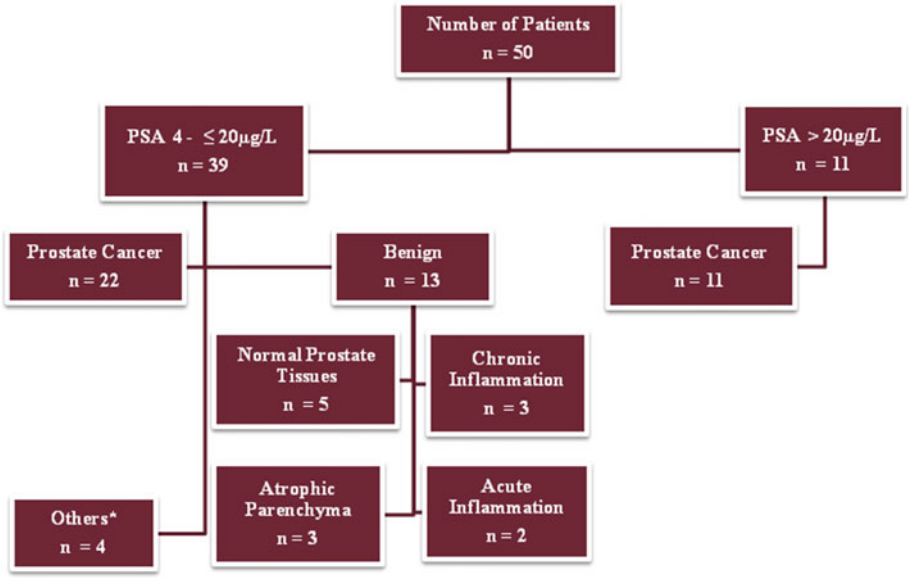

Fig. 3 Summary of prostate biopsies, histopathology results (* others include atypia and PIN)

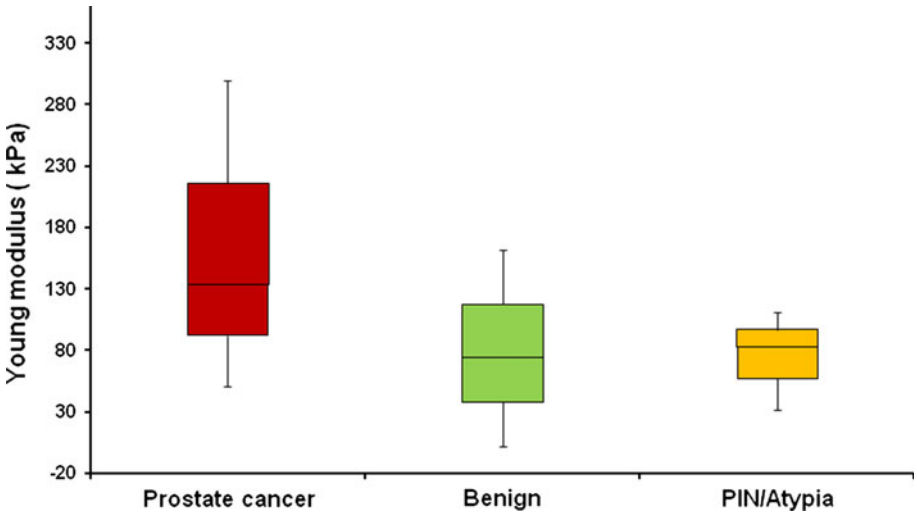

Fig. 4 Whisker plot showing relationship of Young's modulus (in kPa) with pathological outcomes

Young's modulus (±SD) values were also matched with the Gleason scores (Table 1; Fig. 5). It was observed that the mean Young's modulus was higher in prostate cores with a Gleason score of 7 (163 ± 63 kPa) than in those with a Gleason score of 6 (95 ± 28.5 kPa). This difference was statistically significant ($p = 0.007$). The mean Young's modulus of Gleason 8 cores was 113 ± 20 kPa; however, this was not statistically different ($p > 0.05$) from Gleason score 6 and 7 cores.

Biopsy core level analysis

Patients with PSA 4–20 µg/L (n = 39)

Fifty patients had all 12 regions of their prostates biopsied. Each region was biopsied using grey scale and had images stored for SWI. A total of 485 cores were obtained (13 cores in 17 patients and 12 cores in 22 patients). The correlation of SWI with the histopathology data showed

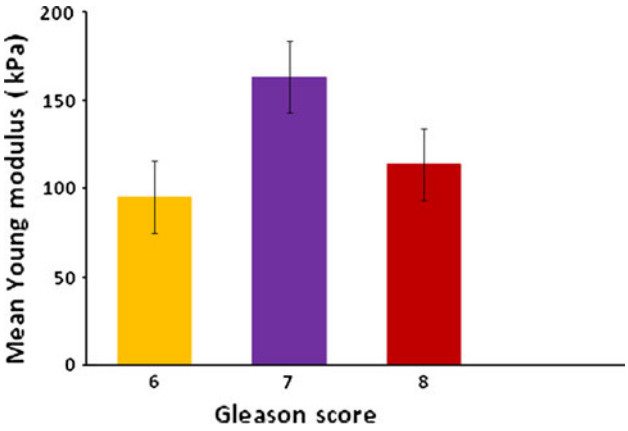

Fig. 5 Relationship of Gleason score with the mean Young's modulus (kPa) value

that 286 cores were correctly identified as abnormal foci on SWI and correlated with cancers on histopathology. One hundred fifty cores were correctly identified as benign on SWI. Twenty-nine cores appeared to be normal on SWI and were reported as cancer on histopathology. Twenty lesions appearing as abnormal on SWI were reported as PIN or normal benign tissue. The sensitivity and specificity of SWI were 0.90 [95 % confidence interval (CI) = 0.60–0.69] and 0.88 (95 % CI = 0.82–0.92), respectively. Corresponding positive and negative predictive values were 0.93 (95 % CI = 0.89–0.95) and 0.83 (0.77–0.88), respectively. The positive likelihood ratio weighted by prevalence was 14.3 (95 % CI = 9.35–21.8), and the negative likelihood ratio weighted by prevalence was 0.19 (0.138–0.270).

Patients with PSA >20 μg/L (n = 11)

A total of 141 core samples were obtained (13 in 9 patients and 12 in 2 patients). One hundred two malignant cores were identified as abnormal SWI areas and 30 benign cores were identified as normal. There were seven cores identified as normal on SWI that were identified as cancer from histopathology. Two cores were identified as abnormal on SWI and reported as benign tissue. The sensitivity and specificity of SWI were 0.93 (95 % CI = 0.86–0.97) and 0.93 (95 % CI = 0.77–0.98), respectively. Corresponding positive and negative predictive values were 0.98 (95 % CI = 0.92–0.99) and 0.81 (0.64–0.91), respectively. The positive likelihood ratio weighted by prevalence was 0.51 (95 % CI = 12.9–201.2), and the negative likelihood ratio weighted by prevalence was 0.23 (0.118–0.460).

Accuracy of SWI imaging in comparison to the distance of abnormality from the transrectal probe position

False-positive results (i.e., where SWI showed abnormal areas but histology reported as benign) or false-negative results (i.e., where SWI showed normal areas but histology reported as cancerous) were observed in the anterior and transition zone of the prostate gland (out of a total of 22 cores that showed a mismatch between SWI and histopathology; 8 cores were from the transitional zone and 9 cores were from the central zone of the prostate).

Discussion

This study assessed the role of SWI in in situ characterisation of areas of the prostate suspected of PCa, addressing a persistent clinical challenge of the low sensitivity and specificity of current grey-scale ultrasound imaging [25, 26]. We have shown that SWI can reliably differentiate between benign and malignant prostate tissue and, in most cases, aid in the real-time targeting of abnormal foci for needle biopsy. The stiffness of cancer foci was 50 % higher than benign tissues with corresponding stiffness values of 133.7 ± 57.6 vs. 74.9 ± 47.3 kPa, respectively. Based on preliminary results in this study, real-time quantitative SWI imaging has a potential to change the clinical practice of PCa identification and screening by improving the localisation of abnormal foci and allowing limited targeted biopsies of suspicious areas, thereby reducing both the complications and the cost associated with the current standard of care (transrectal grey-scale ultrasonography-directed biopsies of the prostate gland). Compared to quasistatic compression elastography, the technique using transrectal SWI is much closer to a standard TRUS clinical examination as it does not require any additional compression. Interestingly, the diagnostic accuracy of SWI in the present study is similar to that of previous reports

Table 1 Relationship of SWI-measured stiffness and Gleason scores of patients with prostate cancer

No. of patients	Gleason score	Maximum (kPa)	Minimum (kPa)	Mean (kPa)	SD
17	3+3	117.1	62.6	95.4	28.5
5	3+4	179.2	126.8	161.1	81.2
7	4+3	216.2	115.7	164.5	50.3
2	4+4	148.2	43.15	108.4	30.9
2	3+5	144.7	95.9	119.1	14.7

[10, 27] despite differences in the reference standards. Barr et al. [10, 27] used sextant biopsies in contrast to the standard 12-core biopsy in the present study. Grey-scale ultrasound characterisation is based on the echogenicity of the gland, which is a nonquantitative method associated with subjective measurements and is invariably dependent on the individual operator's assessment and experience. From a purely technological standpoint, it is not surprising that grey-scale TRUS lacks the ability to differentiate cancer from normal tissues in nearly 50 % of cases [3, 4]. Moreover, there is no specific diagnostic echogenic pattern associated with PCa, and potential improvements utilizing three-dimensional reconstruction remain inconclusive [28, 29]. A recent systematic review summarising the application of elastography in the diagnosis of PCa have highlighted some of these issues [29]. The addition of SWI technology to standard prostate ultrasound appears to address at least some of these technological limitations. Moreover, although SWI provides much needed solutions to the ongoing challenge of accurately locating the areas of interest in the prostate, it also has the inherent advantage of independence from operator experience and expertise. All of these points indicate great potential to change clinical prostate biopsy practice in the future.

Whether SWI can reliably predict the grade of cancer—especially characterise "significant disease" or "indolent lesions" that behave in a benign manner—requires further evaluation. However, in the present study, stiffness values of areas with a Gleason score of 7 PCa were found to be statistically higher than those with Gleason score of 6, while the values of Young's modulus for a Gleason score of 8 fell between scores 6 and 7. Further studies with a larger number of cases are therefore required to determine the exact relationship between the Young's modulus values and tumour grade. A recent report describing SWI for breast cancer imaging suggests that it is quite useful for estimating the aggressiveness of these cancers [30].

Detailed analysis of the false-positive/false-negative cores from the various regions (i.e., where SWI showed a mismatch with the histopathology report) showed that the abnormal areas detected by SWI were located within zones of the prostate where the incidence of PCa is generally low (i.e., 8 cores from the transitional zone and 9 cores from the central zone of the prostate). A smaller mismatch was observed in the peripheral part of the prostate in 5 cores (3 cores from apex and 2 cores from base).

This study highlights the role of SWI stiffness measurement and in situ characterisation of benign and malignant prostatic tissues. Improved technologies such as SWI for the guided biopsy of the prostate remain the main focus of ultrasound imaging innovations. Innovation and improvement in this field may help to more effectively and objectively place a biopsy needle into the suspicious site within the prostate gland. In addition, quantitative tissue stiffness measurement and its correlation with grade of cancer is an interesting finding. Further research is ongoing in this area and is expected to shed more light on this issue of crucial importance. Most importantly, early and accurate detection of PCa may better guide minimally invasive therapy and may therefore offer an increasingly plausible alternative to radical surgery that is currently directed at the entire prostate gland.

The study is limited by the relatively small number of participants in the preliminary observation. In addition, it was limited to a single-centre so the number of observers and operators was relatively small as well. Findings of additional biopsies directed by SWI could be subject to selection and confirmation biases in the absence of a similar number of systematic biopsies in the control arm using grey-scale ultrasonography. However, our promising preliminary results strongly underscore the importance of designing a multicentre study with a larger cohort of patients. If our current findings stand in expanded context, the next logical step could be to determine how best to use SWI to differentiate "significant "and "indolent" prostate cancers. Future research in this emerging technology has to be conducted using established diagnostic accuracy methodology and a reference standard. Although histology of radical prostatectomy specimens would be an ideal reference standard, 12-core biopsy is a reasonable second best option. Most certainly, sextant biopsies used as a reference standard, as in a previous report [10], are subject to detection bias. Moreover, sextant biopsy protocols are obsolete now and are not the basis of current urology practice.

Acknowledgments The authors thank SuperSonic Imagine (Aix-en-Provence, France) for an equipment grant to support this work.

Disclosures The authors have no conflicts of interest or financial ties to disclose.

References

1. Frauscher F, Gradl J, Pallwein L (2005) Prostate ultrasound–for urologists only? Cancer Imaging 5 Spec No A:S76–82
2. Aigner F, Pallwein L, Schocke M, Lebovici A, Junker D, Schafer G, Mikuz G, Pedross F, Horninger W, Jaschke W, Halpern EJ, Frauscher F (2011) Comparison of real-time sonoelastography with T2-weighted endorectal magnetic resonance imaging for prostate cancer detection. J Ultrasound Med 30:643–649
3. Ginat DT, Destounis SV, Barr RG, Castaneda B, Strang JG, Rubens DJ (2009) US elastography of breast and prostate lesions. Radiographics 29:2007–2016
4. Spârchez Z (2011) Real-time ultrasound prostate elastography. An increasing role in prostate cancer detection? Med Ultrason 13:3–4
5. Oehr P, Bouchelouche K (2007) Imaging of prostate cancer. Curr Opin Oncol 19:259–264

6. Krouskop TA, Wheeler TM, Kallel F, Garra BS, Hall T (1998) Elastic moduli of breast and prostate tissues under compression. Ultrason Imaging 20:260–274
7. Zhai L, Polascik TJ, Foo WC, Rosenzweig S, Palmeri ML, Madden J, Nightingale KR (2012) Acoustic radiation force impulse imaging of human prostates: initial in vivo demonstration. Ultrasound Med Biol 38:50–61
8. Curiel L, Souchon R, Rouviere O, Gelet A, Chapelon JY (2005) Elastography for the follow-up of high-intensity focused ultrasound prostate cancer treatment: initial comparison with MRI. Ultrasound Med Biol 31:1461–1468
9. Evans A, Whelehan P, Thomson K, McLean D, Brauer K, Purdie C, Jordan L, Baker L, Thompson A (2010) Quantitative shear wave ultrasound elastography: initial experience in solid breast masses. Breast Cancer Res 12:R104
10. Barr RG, Memo R, Schaub CR (2012) Shear wave ultrasound elastography of the prostate: initial results. Ultrasound Q 28: 13–20
11. Bercoff J, Chaffai S, Tanter M, Sandrin L, Catheline S, Fink M, Gennisson JL, Meunier M (2003) In vivo breast tumor detection using transient elastography. Ultrasound Med Biol 29:1387–1396
12. Bercoff J, Pernot M, Tanter M, Fink M (2004) Monitoring thermally-induced lesions with supersonic shear imaging. Ultrason Imaging 26:71–84
13. Nelson ED, Slotoroff CB, Gomella LG, Halpern EJ (2007) Targeted biopsy of the prostate: the impact of color Doppler imaging and elastography on prostate cancer detection and Gleason score. Urology 70:1136–1140
14. Sebag F, Vaillant-Lombard J, Berbis J, Griset V, Henry JF, Petit P, Oliver C (2010) Shear wave elastography: a new ultrasound imaging mode for the differential diagnosis of benign and malignant thyroid nodules. J Clin Endocrinol Metab 95:5281–5288
15. Sarvazyan A, Hall TJ, Urban MW, Fatemi M, Aglyamov SR, Garra BS (2011) An overview of elastography—an emerging branch of medical imaging. Curr Med Imaging Rev 7:255–282
16. Urban MW, Alizad A, Aquino W, Greenleaf JF, Fatemi M (2011) A review of vibro-acoustography and its applications in medicine. Curr Med Imaging Rev 7:350–359
17. Parker KJ, Doyley MM, Rubens DJ (2011) Imaging the elastic properties of tissue: the 20 year perspective. Phys Med Biol 56:R1–R29
18. Krouskop TA, Dougherty DR, Vinson FS (1987) A pulsed Doppler ultrasonic system for making noninvasive measurements of the mechanical properties of soft tissue. J Rehabil Res Dev 24:1–8
19. Garra BS (2011) Elastography: current status, future prospects, and making it work for you. Ultrasound Q 27:177–186
20. Ophir J, Cespedes I, Ponnekanti H, Yazdi Y, Li X (1991) Elastography: a quantitative method for imaging the elasticity of biological tissues. Ultrason Imaging 13:111–134
21. Ophir J, Garra B, Kallel F, Konofagou E, Krouskop T, Righetti R, Varghese T (2000) Elastographic imaging. Ultrasound Med Biol 26(Suppl 1):S23–S29
22. Varghese T (2009) Quasi-static ultrasound elastography. Ultrasound Clin 4:323–338
23. Tanter M, Bercoff J, Athanasiou A, Deffieux T, Gennisson JL, Montaldo G, Muller M, Tardivon A, Fink M (2008) Quantitative assessment of breast lesion viscoelasticity: initial clinical results using supersonic shear imaging. Ultrasound Med Biol 34: 1373–1386
24. Delahunt B, Miller RJ, Srigley JR, Evans AJ, Samaratunga H (2012) Gleason grading: past, present and future. Histopathology 60:75–86
25. Aigner F, Mitterberger M, Rehder P, Pallwein L, Junker D, Horninger W, Frauscher F (2010) Status of transrectal ultrasound imaging of the prostate. J Endourol 24:685–691
26. Kuligowska E, Barish MA, Fenlon HM, Blake M (2001) Predictors of prostate carcinoma: accuracy of gray-scale and color Doppler US and serum markers. Radiology 220:757–764
27. Barr RG, Destounis S, Lackey LB 2nd, Svensson WE, Balleyguier C, Smith C (2012) Evaluation of breast lesions using sonographic elasticity imaging: a multicenter trial. J Ultrasound Med 31:281–287
28. Garg S, Fortling B, Chadwick D, Robinson MC, Hamdy FC (1999) Staging of prostate cancer using 3-dimensional transrectal ultrasound images: a pilot study. J Urol 162:1318–1321
29. Aboumarzouk OM, Ogston S, Huang Z, Evans A, Melzer A, Stolzenberg JU, Nabi G (2012) Diagnostic accuracy of transrectal elastosonography (TRES) imaging for the diagnosis of prostate cancer: a systematic review and meta-analysis. BJU Int 110(10): 1414–1423; discussion 1423
30. Evans A, Whelehan P, Thomson K, McLean D, Brauer K, Purdie C, Baker L, Jordan L, Rauchhaus P, Thompson A (2012) Invasive breast cancer: relationship between shear-wave elastographic findings and histologic prognostic factors. Radiology 263: 673–677